



Optimization of Thermal Conductivity of NanoPCM-Based Graphene by Response Surface Methodology

Open
Access

Navid Aslfattahi^{1,*}, Alireza Zandehboudi², Saidur Rahman^{3,4,*}, Mohd Faizul Mohd Sabri^{1,^}, Suhana Mohd Said⁵, A. Arifutzzaman³, Nor Azwadi Che Sidik⁶

¹ Department of Mechanical Engineering, Faculty of Engineering, University of Malaya, 50603, Kuala Lumpur, Malaysia

² Department of Energy and Process Engineering, Norwegian University of Science and Technology (NTNU), NO-7491 Trondheim, Norway

³ Research Center for Nano-Materials and Energy Technology (RCNMET), School of Science and Technology, Sunway University, Bandar Sunway, Petaling Jaya, 47500, Selangor Darul Ehsan, Malaysia

⁴ Department of Engineering, Lancaster University, Lancaster, LA1 4YW, United Kingdom

⁵ Department of Electrical Engineering, Faculty of Engineering, University of Malaya, 50603, Kuala Lumpur, Malaysia

⁶ Malaysia – Japan International Institute of Technology (MJIIT), University Teknologi Malaysia, Jalan Sultan Yahya Petra, 54100 Kuala Lumpur, Malaysia

ARTICLE INFO

ABSTRACT

Article history:

Received 3 June 2020

Received in revised form 7 July 2020

Accepted 15 July 2020

Available online 25 September 2020

Common phase change materials (PCMs) possess very low thermal conductivity whilst hybrid PCM with graphene filler could be produced to achieve increased thermal conductivity. This research focuses on the effects of graphene flakes on the thermal conductivity of a PCM (paraffin wax). Three experimental parameters at different levels of average lateral sizes of graphene flakes (4.5, 5 and 7 μ m), mass fractions (0.1, 0.2 and 0.25 wt.%), and rising temperatures (25-75°C) are considered. For the first time in the literature, the impact of various parameters on the thermal conductivity performance of the nanoPCM-based graphene nano-composites is investigated extensively by adopting response surface methodology supported by central composite design. Thermal conductivity prediction is proposed by a new general correlation and a promising value of the coefficient of determination (R²) higher than 0.88. Amongst the investigated various variables in terms of impact on thermal conductivity, the temperature is identified as the most influential parameter on response variables. According to the implemented optimization technique, for the composite with the average graphene flake size of 4.5 μ m, the optimum value of the thermal conductivity is found 0.275 W/m K at the mass fraction of 0.186 wt.% and temperature of 69.73°C.

Keywords:

NanoPCM; Response Surface Methodology; 2FI Model; Thermal Conductivity; Desirability Function

Copyright © 2020 PENERBIT AKADEMIA BARU - All rights reserved

* Corresponding author.

E-mail address: navid.fth87@yahoo.com

* Corresponding author.

E-mail address: saidur@sunway.edu.my

^ Corresponding author.

E-mail address: faizul@um.edu.my

<https://doi.org/10.37934/arfmts.75.3.108125>

1. Introduction

Thermal conductivity is considered as a significant key factor in high-tech engineering sectors. Thermal conductivity of the cooling fluids is the most crucial parameter accountable for the enhanced heat transfer [1]. The application of water, ethylene glycol and engine oils as traditional heat transfer fluids (HTFs) in modern high-tech industries is limited due to the low thermo-physical properties. Their inherently very poor thermal conductivity and adverse effect of phase incompatibility influence the process efficiency of the system [2,3]. PCMs are applicable in energy storage for the systems with low energy density [4,5]. In the past few years, PCMs have been considered as a substitute cooling material in various applications [6,7]. Low thermal conductivity is significant issue in majority of the PCMs despite that high levels of energy storage is the privileges of these materials [8-10]. In the past four decades, numerous PCMs, with distinctive phase transitions (e.g. solid–liquid, solid–solid) have been produced broadly [11,12]. Different inorganic and organic substances are utilized for the formation of required PCMs [13]. The most promising PCMs utilized in low-temperature applications (<100 °C) are paraffin waxes due to their low vapour pressure of melt and chemical inertness, high latent heat of fusion and negligible super-cooling [14,15]. Currently, paraffin waxes are considered as a supreme choice for arrangement of smart PCMs for diverse applications. Energy harvesting of solar energy systems, improving the performance of electronic devices, thermal comfort in vehicles are some aspects of usefulness of PCMs [16,17]. The desire of the higher enhancements of thermal conductivity of the PCMs heads toward generating the idea of adding carbon-based nano-materials to produce composites for the better enhancement of thermal conductivity. Hexagonal carbon structured few layered graphene attracted its implication in heat transfer applications because of their extremely high thermo-physical properties. Carbon based nano-materials are well-known for the supreme specific surface area (SSA) with negligible thickness of the layers [18,19]. Fukai *et al.*, [20] reported that the effective thermal conductivity of the paraffin wax induced with 2% carbon fibers could be increased by a factor of six. In another study, the addition of MWCNT to paraffin wax revealed the increment of 35% in thermal conductivity of the prepared nano-composites in solid state [21]. Fan *et al.*, [22] evaluated the effects of variety types of carbon fillers on thermal properties of paraffin-based phase change materials. They reported 164% enhancement in the thermal conductivity of PCM/graphene nanoplatelets (GNPs) with loading concentration of 5 wt.% of GNP nanoparticles. In a study conducted by Yu *et al.*, [23], the effects of the size and shape of various nanocarbon fillers on thermal conductivity of the liquid paraffin-based nanocomposites was evaluated extensively. Combination of prevalent properties with the effortlessness of fabrication of polymer composites with the addition of graphene flakes is imperative in numerous applications such as electronic industry and sensors [24]. Processing criterion such as mass fraction of filler, particle size and temperature affect significantly final properties of the composites [25]. Correlating these processing parameters is critical to adapt the composites for a particular application. Modelling of these correlations consists of the mathematical understanding from experimental data. Mathematical models in terms of cost effectiveness and reducing the experimental works for the purpose of designing the composites are considered as attractive methods. Computational methods can effectively select the proper PCM and comprehend its characteristics. A conventional system processes the factors independently and specifies their effects on output parameters in spite of that, a productive computational analysis is able to specify its ideal applicability to increase the entire system applicability [26]. The conventional framework is time consuming and inefficient as the inter-related effects among the parameters are not considered. Response surface methodology (RSM) is an important way to deal with the restrictions of experimental efforts and to assess the productivity of these frameworks. A group of mathematical and statistical methodologies are included which are

beneficial for modelling, optimization and specifying the impacts of multiple independent parameters on dependent variables and the inter-related impacts among them. In addition, this process provides optimized procedure with a restricted number of experimental information. Jamekhorshid *et al.*, [27] implemented response surface methodology for analysis and statistical design of the microencapsulated PCM to evaluate the average particle size and melting latent heat. Sheikholeslami *et al.*, [28] applied RSM to evaluate the performance of latent heat thermal energy storage systems (LHTESS), including PCMs during release (discharging) procedure. The results of hybrid framework of two-factor model and desirability function would cause to have better overview of different dominant variables. The significance of this framework can be highlighted during designing, optimizing and enhancing the thermal conductivity of nanoPCM-based graphene composite apart from any experimental work.

However, to the best of authors' knowledge, none of the previous research works has evaluated the thermal conductivity of nanoPCM-based graphene composite performance under different conditions. Besides, there is no systematic methodology for the parametric optimization of the nanoPCM-based graphene composites towards higher thermal conductivity. The optimization and simulation of experimental variables cause to acquire satisfactory levels of operating conditions towards the desired outputs, where they will not be influenced by variations in the factor setting. Consequently, this paper aims to assess the thermal conductivity of nanoPCM-based graphene composites by comprehensively evaluating the impact of influential variables and subsequently optimizing them. Therefore, in this work, central composite design (CCD) and response surface methodology (RSM) are adopted to perform the experimental validation and modelling of the nanoPCM-based graphene nano-composites. Achieving concise set of data is the main advantage of employing RSM-CCD to determine the optimum conditions with a low number of runs.

2. Materials and Methods

Three different types of multi-layered graphene flake with the average lateral flake size of 4.5 μm (AO-3, purity 99.2%), 5 μm (AO-2, purity 99.9%) and 7 μm (AO-4, purity 98.5%) were supplied by Graphene Supermarket. Graphene flakes were used as received. Pure Paraffin Wax (PW70) was used as PCM supplied by Phase Change Materials Products Ltd.

2.1 Preparation of NanoPCM-based Graphene Composites

Mass of PCM (PW70) and graphene flakes were measured using a microbalance (TX323L, UNIBLOC). For every type of graphene, three different compositions were prepared with the variation of graphene mass fraction 0.1, 0.2 and 0.25 wt.%, respectively in the PW70 base material. Afterward the acquired composites were added into the beaker. Due to change of melting point of PW70, a hot plate (IKA, C-MAG HS7 digital) was used during mixture. The mixtures were then stirred using a magnetic stirrer for two hours within the rising temperature ranging from 70 to 100 °C. Acquired nanoPCM composites were poured into the vial for the measurement of thermal conductivity.

2.2 Thermal Conductivity Measurement

In this study, measurement of thermal conductivity is the crucial parameter for analyzing the thermal properties of the prepared nanoPCM-based graphene composites. The measurement of the thermal conductivity was conducted by using a KD2 Pro thermal analyzer (Decagon, USA). The sensor TR-1 (100 mm length and 2.4 mm diameter) was used in these measurements. The temperature-

dependent investigation on the effective thermal conductivity of the prepared samples was conducted using a modern programmable heating water bath of model (DAIHAN Scientific Water Bath-Fuzzy Control System). This water bath was used for controlling the temperature. The accuracy of the utilized water bath was in the range of ± 0.01 °C. Thermal conductivity of the prepared samples was investigated in four specified temperatures (25, 35, 55 and 75 °C). The sample temperature was monitored by locating a thermocouple inside the sample. Before conducting the thermal conductivity measurement, the performance of the sensor was calibrated with the manufacturer suggested material. The obtained accuracy was $\pm 1\%$. Measurement set-up was customized including thermal insulation inside water bath and increasing the reading time of the KD2 Pro to increase the accuracy of thermal conductivity results. Experimental set-up in the laboratory is shown in Figure 1. Thermal conductivity measurements were repeated for several times to assure regarding the consistency of the acquired results. The average values of the measured thermal conductivities were considered for the analysis. A certain percentage of the data was ignored considering them as outliers. The measurement errors in these measurements were found from ± 0.003 to ± 0.007 . This range demonstrated the high reliability and accuracy of the conducted experimental data.

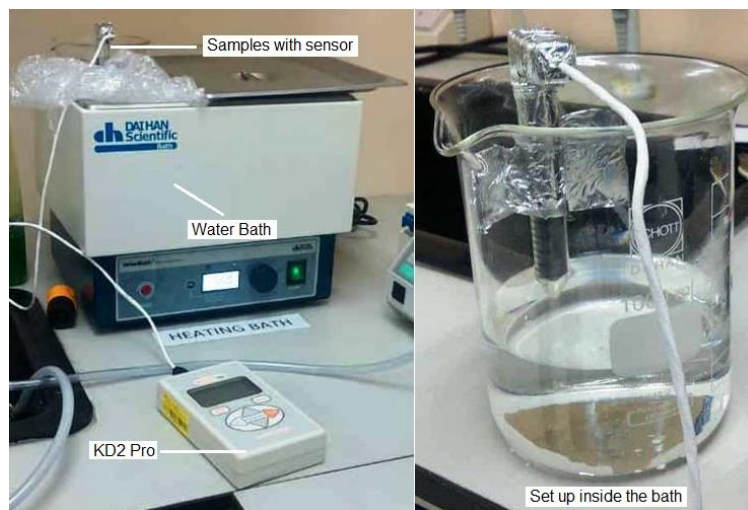


Fig. 1. Experimental setup of thermal conductivity measurement instruments

2.3 Response Surface Methodology

Response surface methodology includes a group of statistical and mathematical methodologies for implementing the empirical models to comprehend the interactional impacts among the parameters for their optimizations [29]. Purpose of this method is to establish an appropriate relation among the response or output variable with the aid of experimental data. These parameters will be applied to the input variables to elucidate the interactional impacts between them [30]. The Eq. (1) demonstrates the relationships among the independent variables such as T , S_p , v and response y as follows

$$y = f(T, S_p, v) + \varepsilon \quad (1)$$

where ε depicts the error in response. The reaction characteristics are symbolized by using a mathematical equation through organizing a map between the set of independent variables and the

response. Response surface methodology (conditioned as a linear function) is the most effective model which is given as follows

$$y = b_0 + \sum_{i=1}^z b_i x_i \tag{2}$$

A 2FI or quadratic polynomial models are considered to match the records for discovering the crucial points, if the primary-order model is insignificant due to the curvature. The 2FI model can be formulated as follows

$$y = b_0 + \sum_{i=1}^z b_i x_i + \sum_{j>i}^z b_{ij} x_i x_j \tag{3}$$

Sum of all linear, self-interaction and cross-interaction phrases are considered in a quadratic polynomial model among predictors. Hence, Eq. (4) represents the approximation function as below

$$y = b_0 + \sum_{i=1}^z b_i x_i + \sum_{i=1}^z b_{ii} x_i^2 + \sum_{i=1}^z \sum_{j>1} b_{ij} x_i x_j \tag{4}$$

Eq. (5) and Eq. (6) represent the method of determining the coefficients by solving the linear model ($Y=XB$) for the quadratic polynomial model.

$$Y = \begin{pmatrix} f(x^1) \\ f(x^2) \\ \vdots \\ f(x^n) \end{pmatrix}, X = \begin{pmatrix} 1 & x_1^1 & \dots & x_z^1 & (x_1^1)^2 & \dots & (x_z^1)^2 & x_1^1 x_2^1 & x_1^1 x_3^1 & \dots & x_{z-1}^1 x_z^1 \\ 1 & x_1^2 & \dots & x_z^2 & (x_1^2)^2 & \dots & (x_z^2)^2 & x_1^2 x_2^2 & x_1^2 x_3^2 & \dots & x_{z-1}^2 x_z^2 \\ \vdots & \vdots & \dots & \vdots & \vdots & \dots & \vdots & \vdots & \vdots & \dots & \vdots \\ 1 & x_1^n & \dots & x_z^n & (x_1^n)^2 & \dots & (x_z^n)^2 & x_1^n x_2^n & x_1^n x_3^n & \dots & x_{z-1}^n x_z^n \end{pmatrix} \tag{5}$$

$$B = (b_0, b_i \dots b_z, b_{ii} \dots b_{zz}, b_{12}, b_{13} \dots b_{p-1,p})^T \tag{6}$$

The final solution is depicted by $B = (X'X)^{-1}X'Y$, wherein y is the expected response, b_i shows the linear coefficient for the independent variables (x_i) and b_0 represents the constant coefficient. The different cross-interaction coefficient between the input factors (x_i and x_j) is depicted by b_{ij} . The i th quadratic coefficient for the input factor (x_i) is considered as b_{ii} [31].

Central composite design (CCD) is recognized as the most exquisite response surface methodology [32]. In CCD all data points will be in terms of coded values of the parameters. Three groups of design points are included in a CCD: (i) functional factorial design points which allows the estimation of the cross-interaction and linear terms, (ii) axial points which are the nominated points including all of the parameters set to zero except one parameter that has the value of $\pm\alpha$ for predicting the self-interaction terms effectively and (iii) the points consisting of all levels set to coded level zero (central points) that indicate the presence of curvature in the response. Thus, five levels of each factor including $-\alpha, +\alpha, -1, 1$, and 0 is required for regular central design. With including the number of variable points (z), the design includes, a matrix from factorial points ($\pm 1, \pm 1, \dots, \pm 1$), a matrix from central points ($0, 0, \dots, 0$) and a matrix from axial points of the form ($\pm\alpha, 0, \dots, 0$), ($0, \pm\alpha, \dots, 0$). The axial matrix in demonstrated as in Eq. (7)

$$K = \begin{bmatrix} \alpha & 0 & 0 & \cdots & \cdots & \cdots & 0 \\ -\alpha & 0 & 0 & \cdots & \cdots & \cdots & 0 \\ 0 & \alpha & 0 & \cdots & \cdots & \cdots & 0 \\ 0 & -\alpha & 0 & \cdots & \cdots & \cdots & 0 \\ \vdots & & & & & & \vdots \\ 0 & 0 & 0 & 0 & \cdots & \cdots & \alpha \\ 0 & 0 & 0 & 0 & \cdots & \cdots & -\alpha \end{bmatrix} \quad (7)$$

The orthogonality of the design is associated with the value of α [33]. Rotatable designs allow steady estimation variance in any respect factors. Therefore, determination of the value of α , for a rotatable design with considering the number of factorial points (N) is calculated by Eq. (8)

$$A = (N)^{\frac{1}{4}} \quad (8)$$

Regression model is a strong mathematical method that permits to assess the interactional impacts between two or more parameters of interest. Many types of regression models have been used for examining the impact of one or more independent parameters on a dependent variable. In this work three various models such as linear, 2FI and quadratic were developed for the prediction of thermal conductivity of prepared nanoPCM-based graphene composite.

In this study, the estimation of thermal conductivity is performed by a developed linear regression with R^2 of 0.8557. The formula for this regression is shown in Eq. (9)

$$Y_i = h(x_i, w) = w^T x_i \quad (9)$$

The task of this type of regression is to discover the weights to identify the exceptional match for the training records. One method of peaking the fit is to calculate the least square error over data set which was performed using the Eq. (10). Figure 2 expresses block diagram of linear regression model.

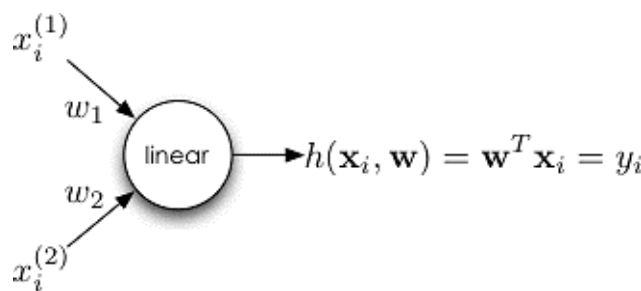


Fig. 2. Regression Model (Linear)

$$L(w) = \sum i(h(x_i, w) - y_i)^2 \quad (10)$$

In order to find the line of best fit, $L(w)$ should be minimized. This model takes as input for a data point with two features $x_i^{(1)}, x_i^{(2)}$ then weights the features with w_1, w_2 followed by summing them and outputs a prediction. Since from the introduction of 2FI in 1920s, statistical interaction detection has been a widely examined term in statistics [34]. Two general approaches have been emerged for conducting interaction detection. One was conducting individual tests for each combination of features [35]. The other one was pre-specifying the all interaction forms of interest then using lasso to simultaneously select the important points [36]. The additive functional form only makes sense, if

the effects of X and Z are theoretically independent. Considering an effortless interactive method including three variables

$$Y = \beta_0 + \beta_1 X + \beta_2 Z + \beta_3 XZ + e_i \tag{11}$$

β_1 and β_2 are commonly (erroneously) referred to as the direct effects of X and Z on Y, and β_3 as the coefficient for the interaction term [37]. With the variables multiplied together the net impact of X on Y is now defined by

$$\begin{aligned} E(Y) &= \beta_0 + \beta_1 X + \beta_2 Z + \beta_3 XZ \\ E(Y) &= \beta_0 + \beta_2 Z + (\beta_1 + \beta_3 Z)X \end{aligned} \tag{12}$$

And the first derivative with respect to X is

$$\frac{\delta E(Y)}{\delta X} = \beta_1 + \beta_3 Z \tag{13}$$

In other words, the marginal impact of X on Y now explicitly depends on the value of Z. Another way of phrasing the expected value function above is

$$E(Y) = \beta_0 + \beta_2 Z + \psi_1 X \tag{14}$$

where $\psi_1 = \beta_1 + \beta_3 Z$ is a “quasi-coefficient” for the marginal impact of X on Y. Likewise with respect to Z

$$\begin{aligned} E(Y) &= \beta_0 + \beta_1 X + (\beta_2 + \beta_3 X)Z \\ &= \beta_0 + \beta_1 X + \psi_2 Z \end{aligned} \tag{15}$$

In this type of interactive model, each interacted covariate’s influence on Y is conditional on the values of the other explanatory variable(s). In this study, among the three different developed models 2FI, caused to best R-squared value. Curvilinear or quadratic relationships for a single variable are also a type of interactive model. For instance, a second-order polynomial regression is depicted as bellow

$$Y = \beta_0 + \beta_1 X + \beta_2 X^2 + e \tag{16}$$

The marginal effect of X on Y is

$$\frac{\delta E(Y)}{\delta X} = \beta_1 + 2\beta_2 X \tag{17}$$

This formula indicates that the marginal effect of X on Y depends linearly on the value of X itself.

2.4 Desirability Function

Desirability is as objective function that ranges from zero (outside of the limits) to one (at the target). The numerical optimization reaches a point that maximizes the desirability function. The characteristics of a target might be changed by modifying the weight of significance [38]. One

desirability function consists of all the combined targets for several factors and responses. A good arrangement of conditions that will meet every one of the goals (not only to achieve a desirability value of 1.0) is the objective of optimization. Desirability is a mathematical strategy to figure out the optimum value. A desirability of 1.0 means, the targets were simply achieved and better results might be available. Consider, making the goals increasingly troublesome or including new criteria for less critical responses and even factors. The definitive target is not to enhance the desirability value. The factor settings that results in the highest desirability values demonstrate there is an island of acceptable outcomes. Desirability curves for goal in Maximum, minimum and target are expressed in Figure 3, Figure 4 and Figure 5.

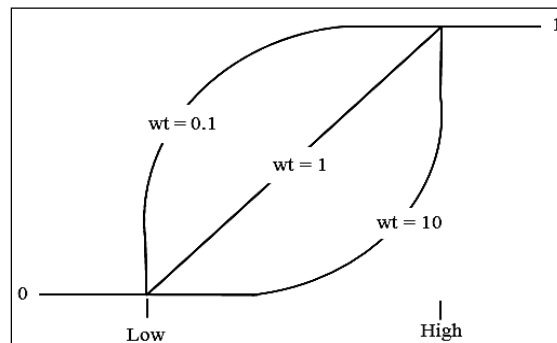


Fig. 3. Desirability curves for goal in maximum

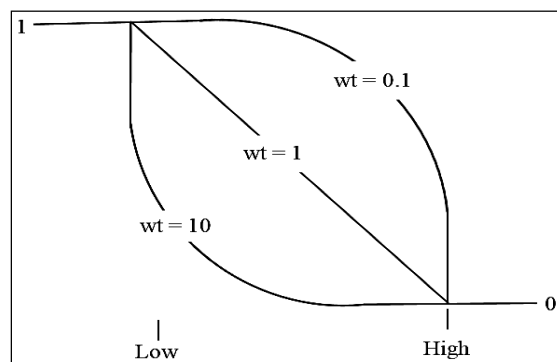


Fig. 4. Desirability curves for goal in minimum

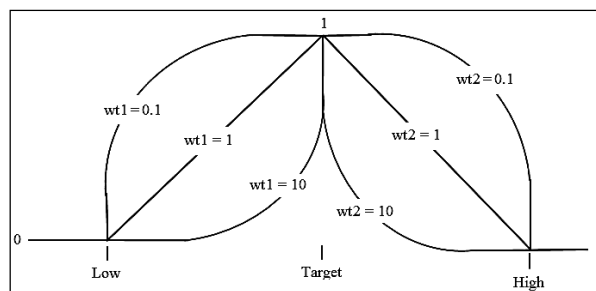


Fig. 5. Desirability curves for goal in target

In the desirability objective function $D(X)$, the importance of each response can be assigned with respect to alternate responses. Significance (r_i) varies from the least important which is a value of 1 to the most important which is a value of 5. The weight field is able to change the shape of desirability for each target. Weights are utilized to provide additional emphasize to the target value. In a linear model, the factor of d_i will be changed from 0 to 1 if the considered weight is 1. More emphasize towards the goal can be achieved with the weights greater than 1 (maximum weight is 10). Weights

less than 1 (minimum weight is 0.1) give less emphasize to the goal. For achieving the maximum value, the desirability will be specified by the following formula

$$d_i = \begin{cases} 0, & Y_i \leq Low_i \\ \left[\frac{Y_i - Low_i}{High_i - Low_i} \right]^{wt_i}, & Low_i < Y_i < High_i \\ 1, & Y_i \geq High_i \end{cases} \quad (18)$$

For goal of minimum, the desirability will be specified by the following formula

$$d_i = \begin{cases} 0, & Y_i \leq Low_i \\ \left[\frac{High_i - Y_i}{High_i - Low_i} \right]^{wt_i}, & Low_i < Y_i < High_i \\ 1, & Y_i \geq High_i \end{cases} \quad (19)$$

For goal as a target within range (constraint), desirability will be defined by the following formulas

$$d_i = \begin{cases} 0, & Y_i \leq Low_i \\ 1, & Low_i < Y_i < High_i \\ 0, & Y_i \geq High_i \end{cases} \quad (20)$$

The desirability function is modified within the program by adding a tail as the function evaluation approaches zero. The tail adjustment is reduced with each iteration to drive the function towards its pure value. Otherwise the optimization would get stuck on the zero desirability planes. Desirability curves for goal as range is expressed in Figure 6.



Fig. 6. Desirability curves for goal as range

3. Results and Discussion

Experimental thermal conductivity of nanoPCM-based graphene composites is plotted in Figure 7 with effect of varying average lateral flake size of graphene flakes and rising temperature. It is seen that at 25°C, the maximum value of thermal conductivity (0.206 W/m K) was perceived for the composite sample with the flake size of 5 μm for the mass fraction of 0.2 wt.%. It was remained same until 35°C. Then, it was enhanced by ~26 and ~30 % at 55 and 75°C respectively compared to 25°C. In contrast, at this temperature the lowest thermal conductivity was detected about 0.202 W/m K for the composite sample of flake size 4.5 μm with the mass fraction of 0.1 wt.%. At 55°C, thermal conductivity was found ~0.223 W/m K (~10 % enhancement) which was enhanced ~36% at 75°C compared to 25°C. Similar phenomenon was observed for the composite sample with the flake size of 7 μm. For this composite, highest thermal conductivity (~0.202 W/m K) was shown for the mass fraction of 0.1 wt.%. The highest thermal conductivity at 25°C was considered to peak the optimum mass fraction for the composites with varying mass fractions of each flake size samples. The

increment of thermal conductivity of this nanoPCM-based graphene composite was due to addition of multi-layered graphene flakes into the PCM (PW70) matrix. Graphene flakes enhanced conductive channels and pathways inside the matrix. Besides, their very high specific surface area with low interfacial thermal resistance between PCM matrix and the flakes provides enormous contribution to increase thermal conductivity of the composite [39-41].

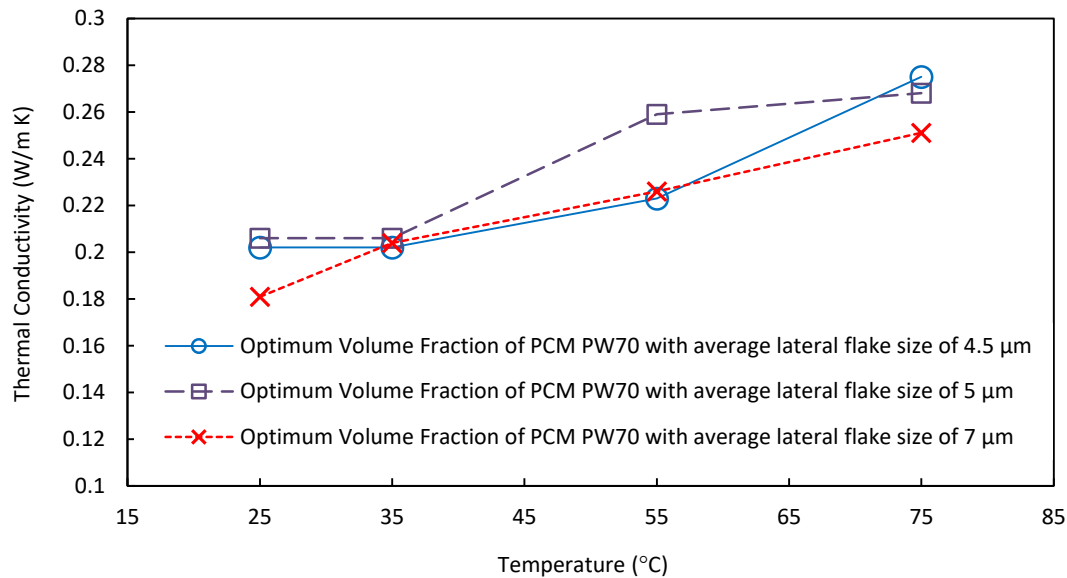


Fig. 7. Effect of rising temperature and average lateral flake size on the thermal conductivity of PCM based graphene composite

Table 1 shows the statistical analysis of the data acquired on the prepared composite samples. Three factors of A, B and C corresponds to the three input parameters of T , S_p , and v respectively. R1, corresponds to the response value of the model.

Table 1

Factor and statistical description of the dataset used for model development

Factor	Name	Units	Minimum	Maximum	Mean	Std. Dev.
A	T	°C	25	75	40	19.4785
B	S_p	μm	4.5	7	5.5	1.11144
C	v	%	0.1	0.25	0.183333	0.0641689
R1	K	W/m K	0.168	0.275	0.212444	0.031805

The calculated values of coefficient of determination (R^2) for the three different models are presented in Table 2. It compares the productivity of each model and guides to choose the most suitable model for the analysis of experimental thermal conductivity of prepared nanoPCM-based graphene composites. The best fitted model is considered for the value of R^2 closer to value of 1. It is seen that, adjusted R^2 value is higher for the 2FI model. 2FI model evidenced as most suitable for the analysis of thermal conductivity under given experimental conditions of nanoPCM-based graphene composites. Therefore, 2FI model is selected for further analysis. The response variable of thermal conductivity in relation to the developed model is presented in Table 3.

Table 2

Accuracy comparison of the linear, 2FI and quadratic models for estimating the thermal conductivity data

Model Summary Statistics			
Source	Std. Dev.	R-Squared	Adjusted R-Squared
Linear	0.013	0.8557	0.8248
2FI	0.014	0.8822	0.8179
Quadratic	0.015	0.8995	0.7864

Table 3

The developed equation of thermal conductivity for the PCM-based graphene composite

K	=
+0.13438	
+2.91183E-003	* T
+9.06754E-003	* S _p
-0.27625	* v
-4.45302E-003	* T * S _p
+5.55347E-003	* T * v
+0.018894	* S _p * v

The interaction and contribution between the design parameters and the corresponding responses was obtained through the analysis of variance (ANOVA). The significance of each model was recognized by the calculation of the probability (p-value). The p-value of less than 0.05 indicates insignificant lack of fit. The ANOVA analysis results for 2FI model is summarized in Table 4.

Table 4

ANOVA analysis results for 2FI model

ANOVA for Response Surface Method				
Source	Sum of Squares	Mean Square	p-value Prorb > F	Result
Model	0.015	2.528E-003	0.0002	Significant
A-T	6.038E-003	6.038E-003	0.0001	Insignificant
B-S _p	3.255E-004	3.255E-004	0.2107	Insignificant
C-v	1.357E-004	1.357E-004	0.4090	Insignificant
AB	4.210E-004	4.210E-004	0.1588	Insignificant
AC	2.251E-004	2.251E-004	0.2926	Insignificant
BC	1.821E-005	1.821E-005	0.7591	Insignificant

Figure 8 illustrates relation of experimentally measured data (actual) and estimated thermal conductivity by developed empirical model of nanoPCM-based graphene composites. Actual thermal conductivity data is placed in the horizontal axis and corresponding predicted values are in the vertical axis. Different coloured square dots constitute the response values at each of the corresponding points. In the plot, red square represents the highest value, while the blue square representing the lowest value. It is clear from the plot that, a fairly good agreement between the anticipated and the real values are perceived. Thereby it confirms the proposed model's viable potential for the implication in practical applications. A value of R² closer to one (0.8822) indicates that the implication interest of developed model is reliable and statistically significant. According to the analysis of sum of squares, linear terms of T, S_p and v showed the contribution of ~84.33, ~4.55 and ~1.9%, respectively. On the other hand, the cross-interaction terms of T-S_p, T-v, and S_p-v bear the

contribution of ~5.88, ~3.14 and ~0.25%, respectively. It indicates the maximum level of importance on the thermal conductivity (Table 4).

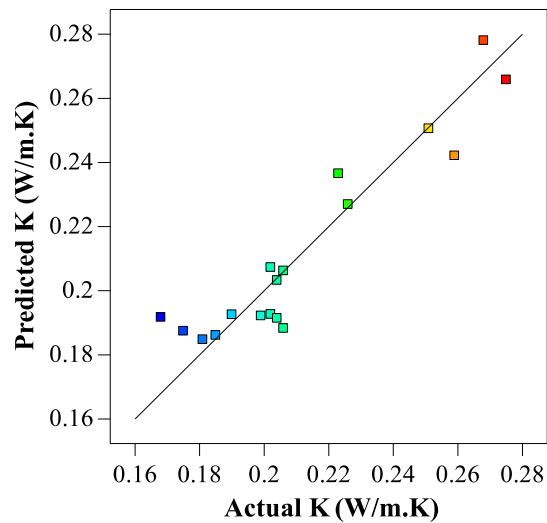


Fig. 8. The relation between the experimental and the predicted thermal conductivity values of PCM based graphene composite

Two-dimensional contour plots of thermal conductivity of nanoPCM-based graphene composite in terms of S_p vs T , V vs T and V vs S_p are presented in Figure 9, Figure 10 and Figure 11, respectively. Figure 9(a) depicts clearly that in small average particle size, high temperature and mass fraction of 0.1 wt.%, the optimum value of thermal conductivity can be acquired. Figure 9(b) shows that lower average particle size in high temperature will cause the high value of thermal conductivity. Besides, Figure 9(c) tends to show the same approach which is totally in accordance with the experimental data. Figure 10. represents the thermal conductivity analysis in terms of V vs T . It demonstrates that the higher mass fraction in high temperature can cause to achieve optimum value of thermal conductivity. Figure 11 illustrates the thermal conductivity analysis in terms of V vs S_p with the different rising temperatures. In Figure 11(a), similar thermal conductivities are observed with varying V and S_p at 25°C. In Figure 11(b) it is obvious that the higher V and lower S_p have caused to achieve the better value of thermal conductivity. Figure 11(c) is in accordance with this approach as well. Figure 12 demonstrates the validity of the counter plots of thermal conductivity. After analyzing the variables, the method of constructing a desirability function based on the responses was applied. The scale of the desirability function ranges from zero (a completely undesirable response) to 1 (a fully desired response).

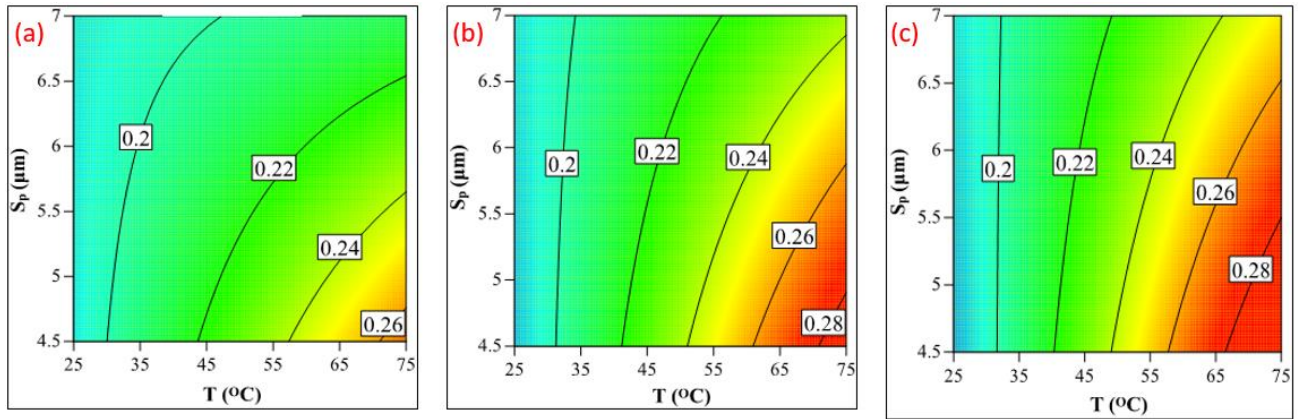


Fig. 9. Contour plots of thermal conductivity in terms of S_p vs. T : (a) $v = 0.1$ wt.%, (b) $v = 0.2$ wt.% and (c) $v = 0.25$ wt.%

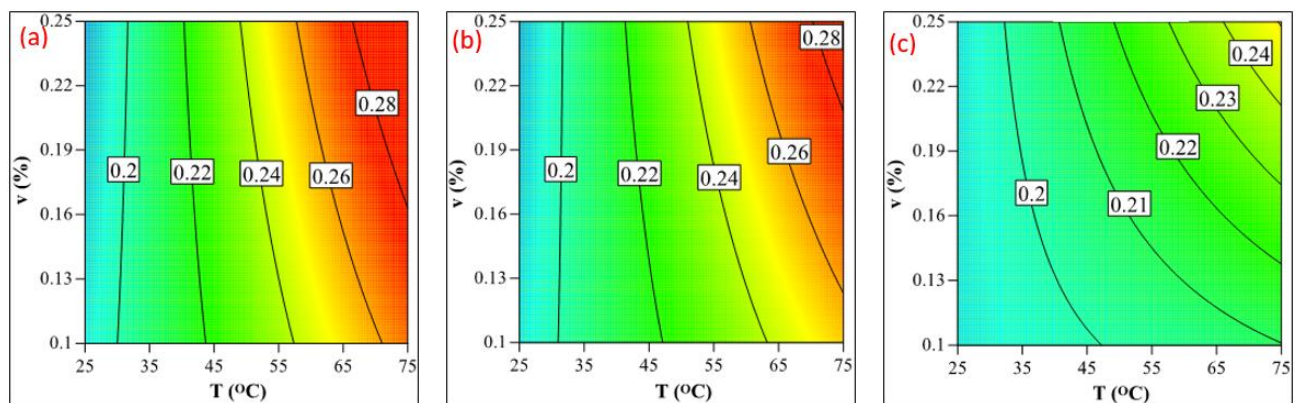


Fig. 10. Contour plots of thermal conductivity in terms of v vs. T : (a) $S_p = 4.5$ μm , (b) $S_p = 5$ μm and (c) $S_p = 7$ μm

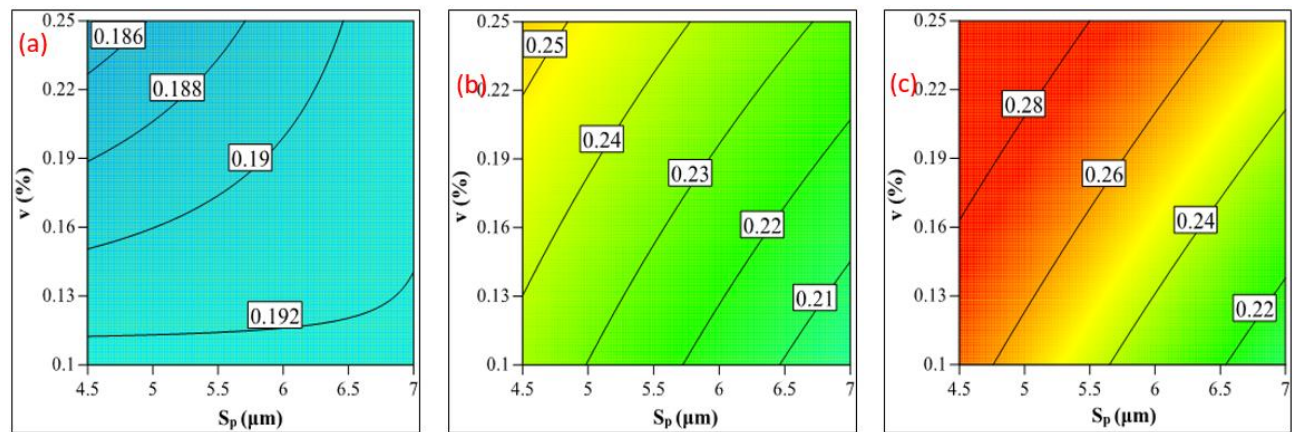


Fig. 11. Contour plots of thermal conductivity in terms of v vs. S_p : (a) $T = 25$ $^{\circ}\text{C}$, (b) $T = 55$ $^{\circ}\text{C}$ and (c) $T = 75$ $^{\circ}\text{C}$

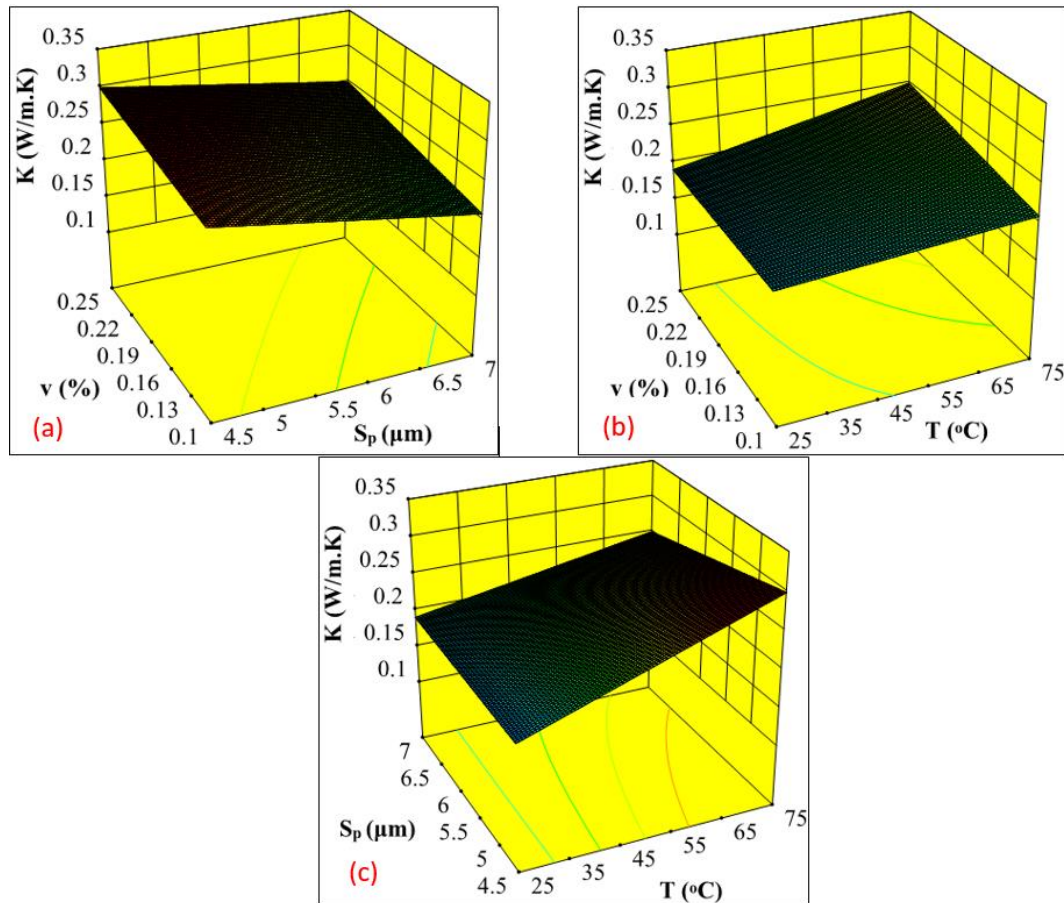


Fig. 12. 3D plots: (a) $T = 75\text{ }^{\circ}\text{C}$, (b) $S_p = 7\text{ }\mu\text{m}$, (c) $v = 5\%$

Graphical ramp views in Figure 13 to Figure 15. expressed the optimized values of the analyzed parameters. According to the implemented optimization technique the optimum parameters of nanoPCM-based graphene composite are obtained. For composite with the average graphene flake size of $4.5\text{ }\mu\text{m}$, the optimum value of V was found $0.186\text{ wt.}\%$ with the thermal conductivity of 0.275 W/m K at 69.73°C . In contrast, for composites with average flake size of $5\text{ }\mu\text{m}$ the optimum V , thermal conductivity and T were found $0.194\text{ wt.}\%$, 0.275 W/m K and 74.19°C , respectively. The optimal values of these parameters were identified $0.25\text{ wt.}\%$ 0.25 W/m K at 75°C for the nanoPCM-based graphene composite with the flake size of $7\text{ }\mu\text{m}$.

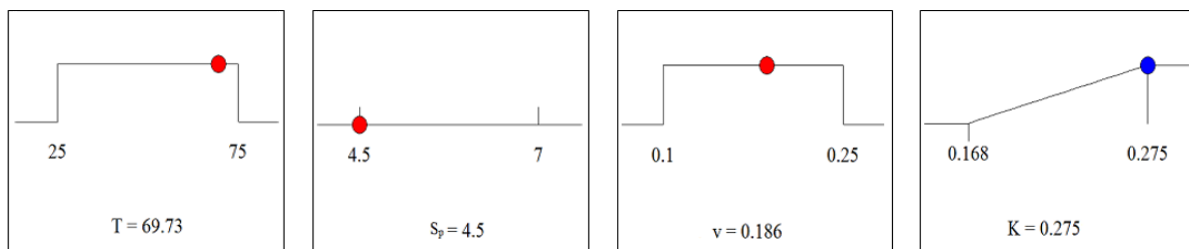


Fig. 13. Graphical ramp views for optimized thermal conductivity: $S_p = 4.5$

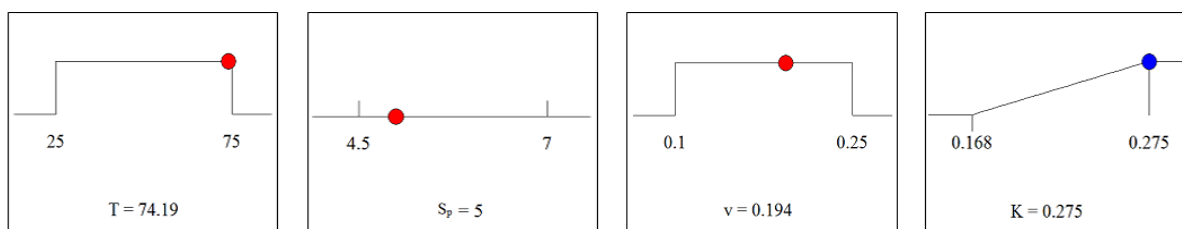


Fig. 14. Graphical ramp views for optimized thermal conductivity: $S_p = 5$

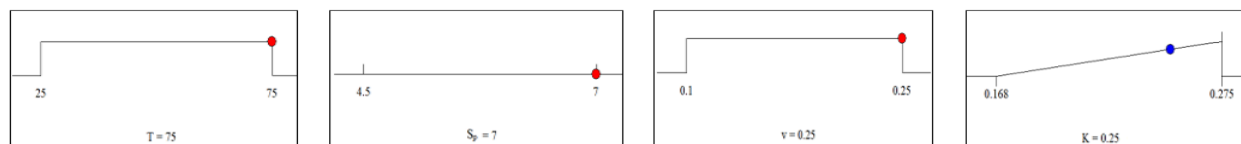


Fig. 15. Graphical ramp views for optimized thermal conductivity: $S_p = 7$

4. Conclusion

In this work, the thermal conductivity of nanoPCM-based graphene composite is investigated. To meet this objective, a test facility to test this material under different conditions is designed, and an empirical model is developed based on response surface methodology. Based on the validated model, the effects of the critical parameters on the thermal conductivity performance of this PCM is elaborated. This model adequately represented by the most critical independent variables, namely average lateral sizes of graphene flakes, mass fractions, and rising temperatures. For the first time in the literature, the results indicate that all independent variables have an influence on the thermal conductivity. Analysis of variance demonstrates that temperature with a contribution of 84.33% is more dominant than the other parameters to affect the thermal conductivity. Besides, the optimal conditions to obtain the higher thermal conductivity are determined. The optimum thermal conductivity value for the composite with the average graphene flake size of 4.5 μm is obtained at the mass fraction of 0.275 W/m K and temperature of 69.73°C.

Acknowledgement

"R. Saidur would like to acknowledge the financial support provided by the Sunway University through the project no# STR-RCTR-RCNMET-001-2019".

References

- [1] Kumar, Periyasamy Mukesh, Jegadeesan Kumar, Rengasamy Tamarasan, Seshachalam Sendhilnathan, and Sivan Suresh. "Review on nanofluids theoretical thermal conductivity models." *Engineering Journal* 19, no. 1 (2015): 67-83.
<https://doi.org/10.4186/ej.2015.19.1.67>
- [2] Siahkamari, Leila, Masoud Rahimi, Neda Azimi, and Maysam Banibayat. "Experimental investigation on using a novel phase change material (PCM) in micro structure photovoltaic cooling system." *International Communications in Heat and Mass Transfer* 100 (2019): 60-66.
<https://doi.org/10.1016/j.icheatmasstransfer.2018.12.020>
- [3] Huang, Yin-Hsien, and Tsung-Eong Hsieh. "Effective thermal parameters of chalcogenide thin films and simulation of phase-change memory." *International Journal of Thermal Sciences* 87 (2015): 207-214.
<https://doi.org/10.1016/j.jthermalsci.2014.08.004>
- [4] Arkar, Ciril, Boris Vidrih, and Sašo Medved. "Efficiency of free cooling using latent heat storage integrated into the ventilation system of a low energy building." *International Journal of Refrigeration* 30, no. 1 (2007): 134-143.
<https://doi.org/10.1016/j.jrefrig.2006.03.009>
- [5] Ali, Hafiz Muhammad. "Experimental investigation on paraffin wax integrated with copper foam based heat sinks for electronic components thermal cooling." *International Communications in Heat and Mass Transfer* 98 (2018): 155-162.

- <https://doi.org/10.1016/j.icheatmasstransfer.2018.08.003>
- [6] Garimella, Suresh V. "Advances in mesoscale thermal management technologies for microelectronics." *Microelectronics Journal* 37, no. 11 (2006): 1165-1185.
<https://doi.org/10.1016/j.mejo.2005.07.017>
- [7] Nayak, K. C., S. K. Saha, K. Srinivasan, and P. Dutta. "A numerical model for heat sinks with phase change materials and thermal conductivity enhancers." *International Journal of Heat and Mass Transfer* 49, no. 11-12 (2006): 1833-1844.
<https://doi.org/10.1016/j.ijheatmasstransfer.2005.10.039>
- [8] Farid, Mohammed M., Amar M. Khudhair, Siddique Ali K. Razack, and Said Al-Hallaj. "A review on phase change energy storage: materials and applications." *Energy Conversion and Management* 45, no. 9-10 (2004): 1597-1615.
<https://doi.org/10.1016/j.enconman.2003.09.015>
- [9] Hosseinizadeh, S. F., AA Rabienataj Darzi, and F. L. Tan. "Numerical investigations of unconstrained melting of nano-enhanced phase change material (NEPCM) inside a spherical container." *International Journal of Thermal Sciences* 51 (2012): 77-83.
<https://doi.org/10.1016/j.ijthermalsci.2011.08.006>
- [10] Abhat, A. "Experimental investigation and analysis of a honeycomb-packed phase change material device." In *11th Thermophysics Conference*, p. 437. 1976.
<https://doi.org/10.2514/6.1976-437>
- [11] Sabbah, Rami, R. Kizilel, J. R. Selman, and S. Al-Hallaj. "Active (air-cooled) vs. passive (phase change material) thermal management of high power lithium-ion packs: Limitation of temperature rise and uniformity of temperature distribution." *Journal of Power Sources* 182, no. 2 (2008): 630-638.
<https://doi.org/10.1016/j.jpowsour.2008.03.082>
- [12] Hashempour, Soha, and Mohammad Hassan Vakili. "Preparation and characterisation of nano enhanced phase change material by adding carbon nano tubes to butyl stearate." *Journal of Experimental Nanoscience* 13, no. 1 (2018): 188-198.
<https://doi.org/10.1080/17458080.2018.1502480>
- [13] Karkri, Mustapha, Mohamed Lachheb, Didier Gossard, Sassi Ben Nasrallah, and Mariam A. AlMaadeed. "Improvement of thermal conductivity of paraffin by adding expanded graphite." *Journal of Composite Materials* 50, no. 19 (2016): 2589-2601.
<https://doi.org/10.1177/0021998315612535>
- [14] Hosseini, M. J., M. Rahimi, and R. Bahrampoury. "Experimental and computational evolution of a shell and tube heat exchanger as a PCM thermal storage system." *International Communications in Heat and Mass Transfer* 50 (2014): 128-136.
<https://doi.org/10.1016/j.icheatmasstransfer.2013.11.008>
- [15] Zalba, Belen, Jose Ma Marin, Luisa F. Cabeza, and Harald Mehling. "Review on thermal energy storage with phase change: materials, heat transfer analysis and applications." *Applied Thermal Engineering* 23, no. 3 (2003): 251-283.
[https://doi.org/10.1016/S1359-4311\(02\)00192-8](https://doi.org/10.1016/S1359-4311(02)00192-8)
- [16] Tong, Xinglin, Jamil A. Khan, and et M. RuhulAmin. "Enhancement of heat transfer by inserting a metal matrix into a phase change material." *Numerical Heat Transfer, Part A Applications* 30, no. 2 (1996): 125-141.
<https://doi.org/10.1080/10407789608913832>
- [17] Cai, Yibing, Yuan Hu, Lei Song, Yong Tang, Rui Yang, Yinping Zhang, Zuyao Chen, and WeiCheng Fan. "Flammability and thermal properties of high density polyethylene/paraffin hybrid as a form-stable phase change material." *Journal of Applied Polymer Science* 99, no. 4 (2006): 1320-1327.
<https://doi.org/10.1002/app.22065>
- [18] Gschwander, S., P. Schossig, and H-M. Henning. "Micro-encapsulated paraffin in phase-change slurries." *Solar Energy Materials and Solar Cells* 89, no. 2-3 (2005): 307-315.
<https://doi.org/10.1016/j.solmat.2004.12.008>
- [19] Tinh, Than Xuan, Nguyen Van Chuc, Vincent Jourdain, Matthieu Paillet, Do-Yoon Kim, Jean-Louis Sauvajol, Ngo Thi Thanh Tam, and Phan Ngoc Minh. "Synthesis of individual ultra-long carbon nanotubes and transfer to other substrates." *Journal of Experimental Nanoscience* 6, no. 5 (2011): 547-556.
<https://doi.org/10.1080/17458080.2010.498839>
- [20] Fukai, Jun, Makoto Kanou, Yoshikazu Kodama, and Osamu Miyatake. "Thermal conductivity enhancement of energy storage media using carbon fibers." *Energy Conversion and Management* 41, no. 14 (2000): 1543-1556.
[https://doi.org/10.1016/S0196-8904\(99\)00166-1](https://doi.org/10.1016/S0196-8904(99)00166-1)
- [21] Wang, Jifen, Huaqing Xie, and Zhong Xin. "Thermal properties of paraffin based composites containing multi-walled carbon nanotubes." *Thermochimica Acta* 488, no. 1-2 (2009): 39-42.
<https://doi.org/10.1016/j.tca.2009.01.022>

- [22] Fan, Li-Wu, Xin Fang, Xiao Wang, Yi Zeng, Yu-Qi Xiao, Zi-Tao Yu, Xu Xu, Ya-Cai Hu, and Ke-Fa Cen. "Effects of various carbon nanofillers on the thermal conductivity and energy storage properties of paraffin-based nanocomposite phase change materials." *Applied Energy* 110 (2013): 163-172.
<https://doi.org/10.1016/j.apenergy.2013.04.043>
- [23] Yu, Zi-Tao, Xin Fang, Li-Wu Fan, Xiao Wang, Yu-Qi Xiao, Yi Zeng, Xu Xu, Ya-Cai Hu, and Ke-Fa Cen. "Increased thermal conductivity of liquid paraffin-based suspensions in the presence of carbon nano-additives of various sizes and shapes." *Carbon* 53 (2013): 277-285.
<https://doi.org/10.1016/j.carbon.2012.10.059>
- [24] Balandin, Alexander A., Suchismita Ghosh, Wenzhong Bao, Irene Calizo, Desalegne Teweldebrhan, Feng Miao, and Chun Ning Lau. "Superior thermal conductivity of single-layer graphene." *Nano Letters* 8, no. 3 (2008): 902-907.
<https://doi.org/10.1021/nl0731872>
- [25] Wu, Shuangmao, Guiyin Fang, and Xu Liu. "Thermal performance simulations of a packed bed cool thermal energy storage system using n-tetradecane as phase change material." *International Journal of Thermal Sciences* 49, no. 9 (2010): 1752-1762.
<https://doi.org/10.1016/j.ijthermalsci.2010.03.014>
- [26] Castell, Albert, Martin Belusko, Frank Bruno, and Luisa F. Cabeza. "Maximisation of heat transfer in a coil in tank PCM cold storage system." *Applied Energy* 88, no. 11 (2011): 4120-4127.
<https://doi.org/10.1016/j.apenergy.2011.03.046>
- [27] Jamekhorshid, A., S. M. Sadrameli, and A. R. Bahramian. "Process optimization and modeling of microencapsulated phase change material using response surface methodology." *Applied Thermal Engineering* 70, no. 1 (2014): 183-189.
<https://doi.org/10.1016/j.applthermaleng.2014.05.011>
- [28] Sheikholeslami, Mohsen, Sina Lohrasbi, and Davood Domairry Ganji. "Response surface method optimization of innovative fin structure for expediting discharging process in latent heat thermal energy storage system containing nano-enhanced phase change material." *Journal of the Taiwan Institute of Chemical Engineers* 67 (2016): 115-125.
<https://doi.org/10.1016/j.jtice.2016.08.019>
- [29] Khan, Zakir, and Zulfiqar Ahmad Khan. "Experimental and numerical investigations of nano-additives enhanced paraffin in a shell-and-tube heat exchanger: a comparative study." *Applied Thermal Engineering* 143 (2018): 777-790.
<https://doi.org/10.1016/j.applthermaleng.2018.07.141>
- [30] Box, George EP, and Kenneth B. Wilson. "On the experimental attainment of optimum conditions." *Journal of The Royal Statistical Society: Series B (Methodological)* 13, no. 1 (1951): 1-38.
<https://doi.org/10.1111/j.2517-6161.1951.tb00067.x>
- [31] Mäkelä, Mikko. "Experimental design and response surface methodology in energy applications: A tutorial review." *Energy Conversion and Management* 151 (2017): 630-640.
<https://doi.org/10.1016/j.enconman.2017.09.021>
- [32] Myers, Raymond H., Douglas C. Montgomery, and Christine M. Anderson-Cook. *Response surface methodology: process and product optimization using designed experiments*. John Wiley & Sons, 2016.
- [33] Jensen, D. R. "C432. Efficiency comparisons of central composite designs." *Journal of Statistical Computation and Simulation* 52, no. 2 (1995): 177-183.
<https://doi.org/10.1080/00949659508811664>
- [34] Box, George EP, and J. Stuart Hunter. "Multi-factor experimental designs for exploring response surfaces." *The Annals of Mathematical Statistics* 28, no. 1 (1957): 195-241.
<https://doi.org/10.1214/aoms/1177707047>
- [35] Fisher, Ronald Aylmer. "Statistical methods for research workers." In *Breakthroughs in Statistics*, pp. 66-70. Springer, New York, NY, 1992.
https://doi.org/10.1007/978-1-4612-4380-9_6
- [36] Lou, Yin, Rich Caruana, Johannes Gehrke, and Giles Hooker. "Accurate intelligible models with pairwise interactions." In *Proceedings of the 19th ACM SIGKDD International Conference on Knowledge Discovery and Data Mining*, pp. 623-631. 2013.
<https://doi.org/10.1145/2487575.2487579>
- [37] Bien, Jacob, Jonathan Taylor, and Robert Tibshirani. "A lasso for hierarchical interactions." *Annals of Statistics* 41, no. 3 (2013): 1111.
<https://doi.org/10.1214/13-AOS1096>
- [38] Nakanishi, Masao, and Lee G. Cooper. "Parameter estimation for a multiplicative competitive interaction model-least squares approach." *Journal of Marketing Research* 11, no. 3 (1974): 303-311.
<https://doi.org/10.1177/002224377401100309>

-
- [39] Costa, Nuno Ricardo, and João Lourenço. "Multiresponse problems: desirability and other optimization approaches." *Journal of Chemometrics* 30, no. 12 (2016): 702-714.
<https://doi.org/10.1002/cem.2848>
- [40] Khanam, P. Noorunnisa, M. A. AlMaadeed, Sumaaya AlMaadeed, Suchithra Kunhoth, M. Ouederni, Dan Sun, A. Hamilton, Eileen Harkin Jones, and Beatriz Mayoral. "Optimization and prediction of mechanical and thermal properties of graphene/LLDPE nanocomposites by using artificial neural networks." *International Journal of Polymer Science 2016* (2016).
<https://doi.org/10.1155/2016/5340252>
- [41] Du, Jinhong, and Hui-Ming Cheng. "The fabrication, properties, and uses of graphene/polymer composites." *Macromolecular Chemistry and Physics* 213, no. 10-11 (2012): 1060-1077.
<https://doi.org/10.1002/macp.201200029>